CHAPTER 2

LITERATURE REVIEWS

2.1. Crystal structure and ferroelectricity

In the so-called *dielectric* materials, the constituent atoms are considered to be ionized to a certain degree and are either positively or negatively charged. In such ionic crystals, when an electric field is applied, cations are attracted to the cathode and anions to the anode due to electrostatic interaction. The electron clouds also deform, causing electric dipoles. This phenomenon is known as *electric polarization* of the dielectric, and the polarization is expressed quantitatively as the sum of the electric dipoles per unit volume [C/m^2]. Figure 2.1 shows schematically the origin of the electric polarization. There are four primary contributions: *electronic*, *ionic*, *dipole reorientation-related and space charge*. The degree to which each mechanism contributes to the overall polarization of the material depends on the frequency of the applied field as shown in Fig. 2.2. Electronic polarization can follow alternating fields with frequencies up to THz-PHz (higher than visible light wave) and ionic polarization responds up to GHz-THz (microwave region) is valid only when the applied electric field has a frequency on the order of THz or higher. Permanent dipole reorientation can follow only up to MHz-GHz. This is why ferroelectric materials with permanent dipoles cannot be used for microwave dielectric materials; their

ลิขสิทธิ์มหาวิทยาลัยเชียงใหม่
Copyright© by Chiang Mai University
All rights reserved

permittivities are typically high at low frequencies (kHz), but decrease significantly with increasing applied electric field frequency.

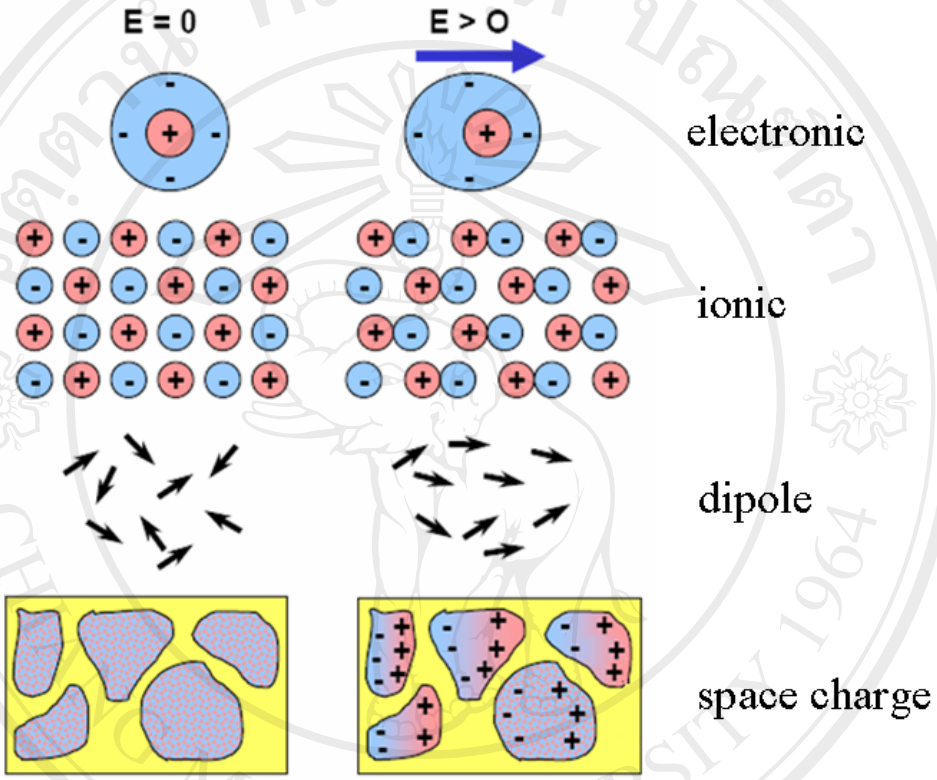

Figure 2.1 Microscopic origins of the electric polarization.

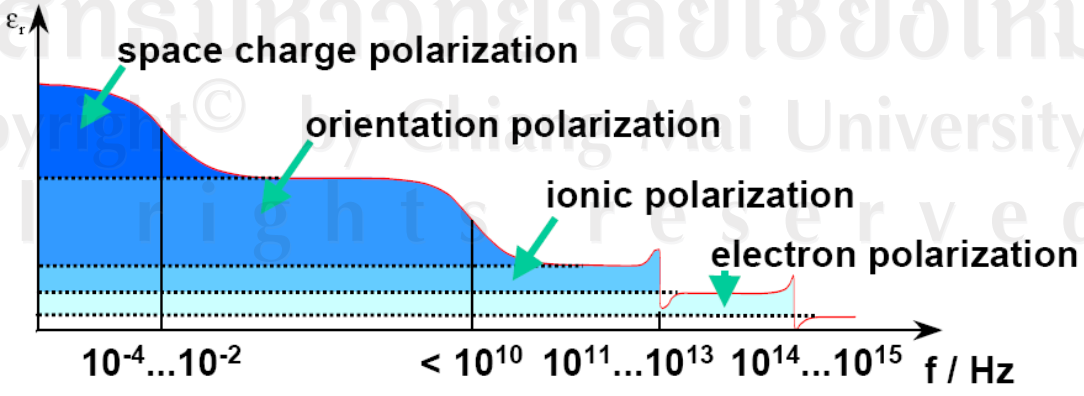

Figure 2.2 Polarization of the material depends on the frequency of the applied field

ลิขสิทธิ์มหาวิทยาลัยเชียงใหม่
Copyright© by Chiang Mai University
All rights reserved

Compared with air-filled capacitors, dielectric capacitors can store more electric charge due to the dielectric polarization **P**. The physical quantity corresponding to the stored electric charge per unit area is called the *electric displacement* **D**, and is related to the electric field **E** by the following expression:

$$\mathbf{D} = \varepsilon_0\mathbf{E} + \mathbf{P} = \varepsilon_r\varepsilon_0\mathbf{E}. \qquad (2.1)$$

where ε_0 is the vacuum permittivity (= 8.854×10^{-12} F/m), ε_r is the material's *relative permittivity* (also simply called permittivity or *dielectric constant*).

Depending on the crystal structure, the centers of the positive and negative charges may not coincide even without the application of an external electric field [6]. Such crystals are said to possess a *spontaneous polarization*. When the spontaneous polarization of the dielectric can be reversed by an electric field, it is called *ferroelectric*. Not every dielectric is a ferroelectric. Crystals can be classified into 32 point groups according to their crystallographic symmetry, and these point groups can be divided into two classes, one with a center of symmetry and the other without one. This classification of the point groups is presented in Table 2.1 [7]. There are twenty-one point groups, which do not have a center of symmetry. Among these, twenty point groups [point group (432) being the sole exception] are *piezoelectric*; that is, positive and negative charges are generated on their surfaces when stress is applied. These materials are known as *piezoelectrics*. *Pyroelectricity* is the phenomenon whereby, due to the temperature dependence of the spontaneous polarization, as the temperature of the crystal is changed, electric charges corresponding to the change of the spontaneous polarization appear on the surface of the crystal. Among the pyroelectric crystals, those whose spontaneous polarization can be reversed by an

ลิขสิทธิ์มหาวิทยาลัยเชียงใหม่
Copyright© by Chiang Mai University
All rights reserved

electric field (not exceeding the breakdown limit of the crystal) are called *ferroelectrics*. There is some experimental ambiguity in this definition. In establishing ferroelectricity, it is necessary to apply an electric field to a pyroelectric material and experimentally ascertain the polarization reversal. Figure 2.3 [8] presents Venn diagram showing how ferroelectrics fit into the different classes of dielectric materials.

Table 2.1 Crystallographic classification scheme based on polarity and the presence of a center of symmetry. [Hex: Hexagonal, Tetra: Tetragonal, Rhomb: Rhombohedral, Ortho: Orthorhombic, Mono: Monoclinic, Tri: Triclinic] [7].

Polar	Symm.	Crystal System										
		Cubic		Hex		Tetra		Rhomb		Ortho	Mono	Tri
Non-Polar (22)	Centro (11)	m3m	m3	6/mmm	6/m	4/mmm	4/m	$\bar{3}m$	$\bar{3}$	mmm	2/m	T
	Non-Centro (21)	432	23	622	$\bar{6}$	422	$\bar{4}$	32		222		
		$\bar{4}3m$		$\bar{6}m2$		$\bar{4}2m$						
Polar (10)				6mm	6	4mm	4	3m	3	2mm	2 m	1

Piezoelectric point groups appear in shaded cells.

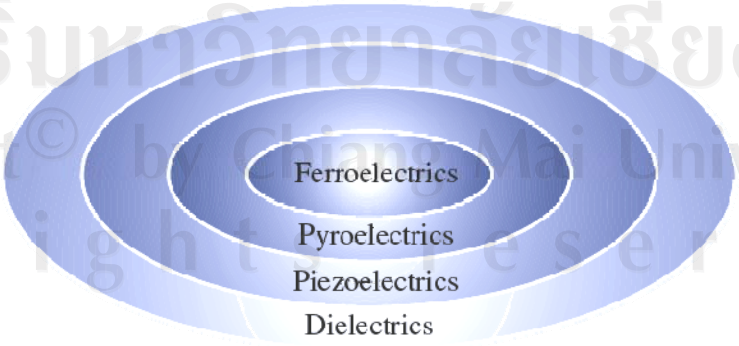

Figure 2.3 Venn diagram of electroceramics properties [8].

ลิขสิทธิ์มหาวิทยาลัยเชียงใหม่
Copyright© by Chiang Mai University
All rights reserved

2.1.1. Normal ferroelectrics

The relation between the net macroscopic polarization of a ferroelectric crystal and the externally applied electric field is given by a hysteresis loop. When an electric field is applied to a ferroelectric, these dipoles can be reoriented with respect to the direction of the applied field. The major difference between ferromagnetic and ferroelectric is the fact that the polarization of the magnetic dipoles in ferromagnetics is attributed to the magnetic dipoles in each individual atom; in ferroelectrics, the polarization is due to the crystal structure as a whole and not of the individual atoms.

As a crystal polarizes, a domain structure is formed. The domain will initially nucleate randomly with their polarization vectors along one of the allowed directions. In order to change the polarization direction, ferroelectric domain walls must be shifted. The driving force for this movement is free energy for the electronic dipole orientation. In ferroelectrics, the dipoles align with the applied electric field and assume a lower energy state compared to that for the spontaneously polarized direction. The energy required to reorient the domains can be seen in the area of the electric displacement versus applied field hysteresis loop, as seen in Fig. 2.4 [8].

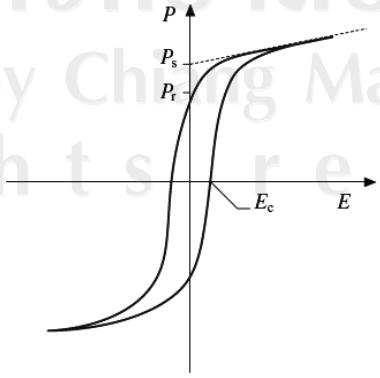

Figure 2.4 A typical ferroelectric hysteresis loop[8].

ลิขสิทธิ์มหาวิทยาลัยเชียงใหม่
Copyright© by Chiang Mai University
All rights reserved

The temperature at which the crystal structure transforms from the paraelectric state into the ferroelectric state is called the Curie point [9]. According to the Curie-Weiss law, the dielectric constant obeys the equation:

$$\frac{1}{\varepsilon} = \frac{(T - T_0)}{C} \tag{2.2}$$

where, C is the Curie-Weiss constant, T is the temperature and, T_o is the Curie-Weiss temperature that is less than T_c. The Curie point is the actual transformation temperature, while the Curie-Weiss temperature is found by extrapolating the plot of the Curie-Weiss law, as shown in Fig. 2.5 [7]. The Curie-Weiss temperature can be as much as ten degrees lower than the Curie point for first-order phase transitions and the two are equal for a second order phase transition. First-order phase transitions are those in which the first derivative of the free energy expansion with respect to temperature is discontinuous as shown in Fig. 2.5(b). In second-order phase transitions, the second derivation is continuous as shown in Fig. 2.5(a).

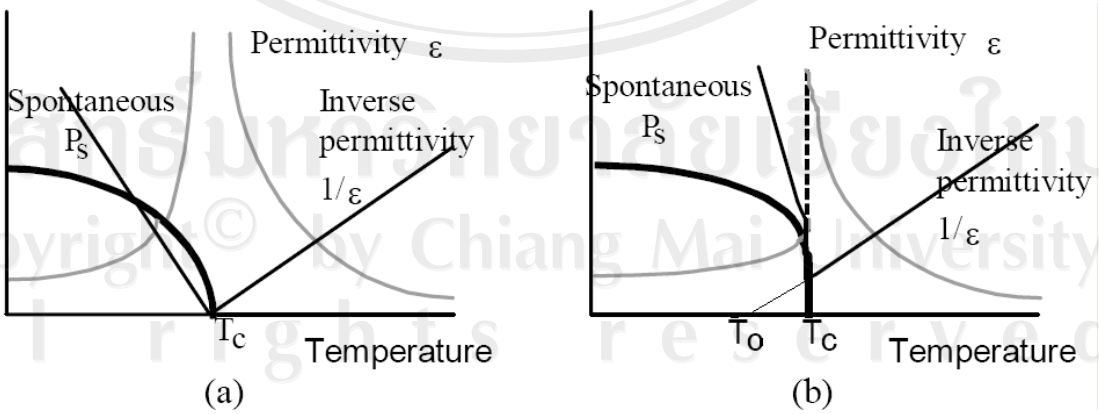

Figure 2.5 A general depiction of the temperature dependences of the spontaneous polarization, the dielectric constant, and the inverse dielectric constant for a ferroelectric (a) second-order phase transitions and (b) first-order phase transitions [7].

ลิขสิทธิ์มหาวิทยาลัยเชียงใหม่
Copyright© by Chiang Mai University
All rights reserved

2.1.2. Relaxor ferroelectrics

The relaxor-ferroelectric behavior of compounds in the complex perovskite family was first reported by Smolenskii *et al.* [4] in the late 1950's. A general formula for the oxide complex perovskite is:

$$\left(A'A''\right)^{XII}(B'B'')^{VI}O_3{}^{VI} \qquad (2.3)$$

where the A' and A'' ions are large cations, generally Pb^{2+}, Ba^{2+}, and Sr^{2+}. The B' ion is an ion with a small charge such as Mg^{2+}, Zn^{2+}, Ni^{2+}, and Fe^{2+}. The B'' ion is a highly charged ion such as Nb^{5+}, Ta^{5+}, W^{4+}, or Ti^{4+}. In this class of materials, the initial discovery of relaxor behavior was reported for the compositions, $Pb(Zn_{1/3}Nb_{2/3})O_3$ [PZN] and $Pb(Mg_{1/3}Nb_{2/3})O_3$ [PMN]. Since Smolenskii's initial work, relaxor behavior has been observed in a large number of complex perovskites and perovskite-related structures. Some general features of relaxor ferroelectrics have been recognized by Cross [10], as shown in Table 2.2

The sharp, well-defined phase transition temperature found for normal ferroelectrics is absent in relaxors. The paraelectric to ferroelectric phase transition becomes broad and diffuse in relaxors and a Curie range replaces the Curie temperature. The permittivity of relaxors is also dispersive in nature at radio frequencies, i.e. the permittivity decreases and the temperature at which the permittivity is at maximum, T_m, shifts to higher temperatures with increasing frequency.

ลิขสิทธิ์มหาวิทยาลัยเชียงใหม่
Copyright© by Chiang Mai University
All rights reserved

In relaxor ferroelectrics, the dielectric constant does not follow Curie-Weiss behavior above the ferroelectric transition, but, instead follows the so-called quadratic Curie-Weiss law[7,11]:

$$\frac{1}{\varepsilon} = \frac{1}{\varepsilon_{max}} + \frac{(T - T_m)^2}{2\delta^2 \varepsilon_{max}} \tag{2.4}$$

where, ε is the real part of the permittivity, ε_{max} is the permittivity at T_m, and δ is the diffuseness parameter. This quadratic relation is valid for materials that display a diffuse phase transition like the relaxor ferroelectric PMN. Most materials, however, show intermediate behavior between the linear and quadratic limits. Uchino[12] addressed this by introducing a variable power law:

$$\frac{1}{\varepsilon} = \frac{1}{\varepsilon_{max}} + \frac{(T - T_m)^\gamma}{2\delta \varepsilon_{max}} \tag{2.5}$$

where γ is the critical exponent of ε. The equation (2.5) can be solved graphically using a log-log plot. A slope of this curve represents the value of the critical exponent, γ, and the intercept gives the diffuseness parameter, δ, according to the following equation:

$$\delta = \left(\frac{e^{-\text{intercept}}}{2\varepsilon_{max}} \right)^{1/\gamma} \tag{2.6}$$

A value of the critical exponent can vary from $\gamma = 1$ for purely normal ferroelectrics, to $\gamma = 2$, for purely relaxor ferroelectrics. The diffuseness parameter is an empirical value that describes the width of the diffuseness phase transition.

ลิขสิทธิ์มหาวิทยาลัยเชียงใหม่
Copyright© by Chiang Mai University
All rights reserved

The relatively rapid decrease of the polarization to zero found in normal ferroelectric at T_c is much more gradual in relaxor ferroelectrics. This gradual decrease extends to temperature above T_m before reaching zero. This can be observed in dielectric hysteresis loops. At temperature below T_m, relaxors show typical *P-E* hysteresis; however, the loops decay slowly into non-linearity as the temperature increases through the Curie range.

The local symmetry of the nano-domains in relaxors is typically rhombohedral. Because of the scale of the nano-domain, optical birefringence and x-ray diffraction measurements do not show anisotropy or line splitting, even far below T_{max}. The global symmetry of relaxors is generally reported as a pseudo-cubic, even in the polar state, due to this ambiguity.

Table 2.2 Property differences between relaxor and normal perovskite ferroelectrics [10].

Property	Normal	Relaxor
Permittivity temperature dependence $\varepsilon = \varepsilon(T)$	Sharp 1st or 2nd order transition about Curie temperature (T_c)	Board-diffuse phase transition about Curie Maxima (T_{max})
Permittivity temperature and frequency dependence $\varepsilon = \varepsilon(T,\omega)$	Weak frequency dependence	Strong frequency dependence
Permittivity behavior in paraelectric range ($>T_C$)	Follow Curie-Weiss law $K = C/(T - T_0)$	Follow Curie-Weiss square law $1/K = 1/K_{max}+(T-T_m)^2/2K_{max}\delta^2$
Remanent polarization	Strong remanent polarization	Weak remanent polarization
Scattering of light	Strong anisotropy (briefringent)	Very weak anisotropy to light (pseudo-cubic)
Diffraction of x-ray	Line splitting owing to spontaneous deformation from paraelectric to ferroelectric phase	No x-ray line splitting giving a pseudo-cubic structure

ลิขสิทธิ์มหาวิทยาลัยเชียงใหม่
Copyright© by Chiang Mai University
All rights reserved

The reasons why these complex perovskites have been investigated intensively for capacitor applications are:

(1) their very high permittivity, and

(2) their temperature - insensitive characteristics (i.e., diffuse phase transition) in comparison with the normal ferroelectric perovskite solid solutions. However, the relaxors exhibit a problem, namely, *dielectric relaxation,* a characteristic highlighted by their name.

High Permittivity

An intuitive crystallographic model (*rattling ion model*) has been proposed to explain the giant permittivity of these disordered perovskites [13]. Figures 2.6(a) and (b) show the ordered and disordered structures for an $A(B^{I}_{1/2}B^{II}_{1/2})O_3$ perovskite crystal. Assuming a rigid ion model, a large "rattling" space is expected for the smaller B ions in the disordered structure [Fig. 2.6(b)] because the large B ions prop open the lattice framework. Much less "rattling" space is expected in the ordered arrangement [Fig. 2.6(a)] where neighboring atoms collapse systematically around the small B ions. When an electric field is applied to a disordered perovskite, the B ions (usually high valence ions) with a large rattling space can shift easily without distorting the oxygen framework. Larger polarization can be expected for unit magnitude of electric field; in other words, larger dielectric constants and larger Curie-Weiss constants should be typical in this case. On the other hand, in ordered perovskites with a very small rattling space, the B ions cannot move easily without distorting the octahedron. A smaller permittivity and a Curie-Weiss constant are expected.

ลิขสิทธิ์มหาวิทยาลัยเชียงใหม่
Copyright© by Chiang Mai University
All rights reserved

Diffuse Phase Transition

The exact reason why the phase transition is diffuse in the relaxor ferroelectrics has not yet been clarified. Uchino [14-16] introduce here the "microscopic composition fluctuation" model which is one of the most widely accepted models for the relaxor ferroelectrics. Within a single *Känzig region* [the minimum polar region size in which cooperative polarization (ferroelectricity) can occur], typically on the order of 10 - 100 nm, the model applied to a $Pb(B^{I}_{1/3}B^{II}_{2/3})O_3$ relaxor assumes a local fluctuation of the B^{I2+} and B^{II5+} ions.

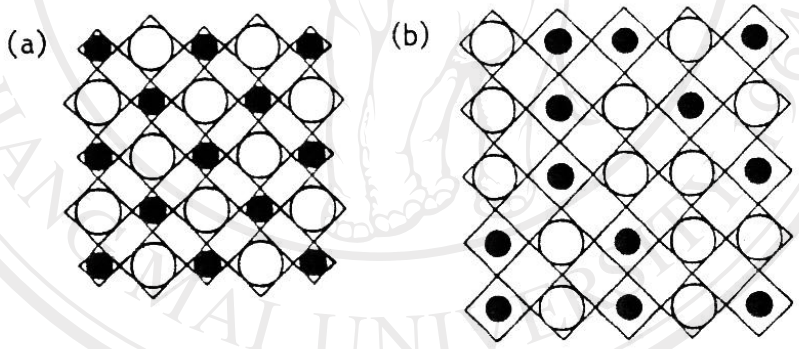

Figure 2.6 Crystal structure models of the $A(B^{I}_{1/2}B^{II}_{1/2})O_3$ type perovskite:(a) the ordered structure with a small rattling space and (b) the disordered structure with a large rattling space [open circle = B^{I} (lower valence cation) and solid circle = B^{II} (higher valence cation)] [13].

ลิขสิทธิ์มหาวิทยาลัยเชียงใหม่
Copyright © by Chiang Mai University
All rights reserved

Dielectric Relaxation

Another significant characteristic of these "relaxor" ferroelectrics is dielectric relaxation (frequency dependence of the permittivity) from which their name is

derived. The temperature dependence of the permittivity for $Pb(Mg_{1/3}Nb_{2/3})O_3$ is plotted in Fig. 2.7 at various measuring frequencies[17].

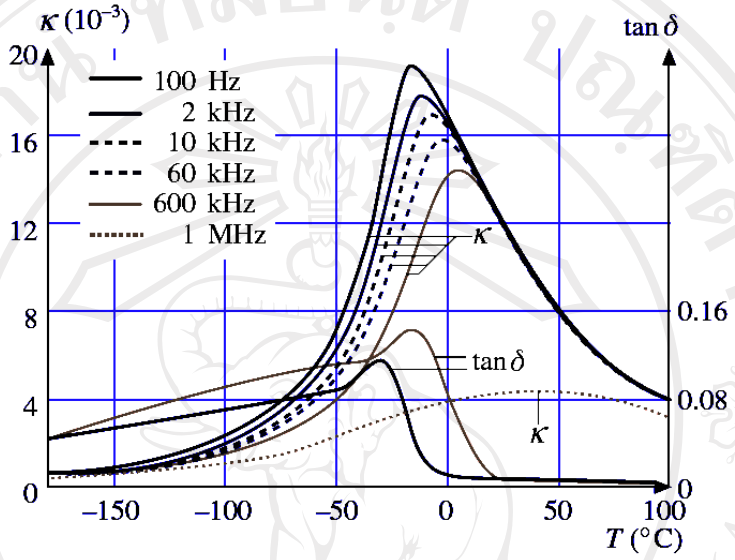

Figure 2.7 The temperature dependence of the permittivity and tan δ in $Pb(Mg_{1/3}Nb_{2/3})O_3$ for the various measuring frequencies from 0.1kHz -1MHz [17].

2.2. Perovskite materials

The perfect prototype perovskite is generally described as having simple cubic structure and takes its name from the isostructural mineral "perovskite" calcium titanate, $CaTiO_3$. However the cubic structure is better described by $SrTiO_3$ [18]. The cubic prototype $SrTiO_3$ has a space group *Pm*3*m* with the titanium atoms located at the corners of the unit cell cube, the strontium atom located at the center of the cube and oxygen atoms are placed at the centers of the twelve cube edges (Fig. 2.8). The first alternative is a cubic cell that has the titanium atom at the center, the strontium atoms are on the cell corners and the oxygen atoms are on the cell faces. The

ลิขสิทธิ์มหาวิทยาลัยเชียงใหม่
Copyright© by Chiang Mai University
All rights reserved

peroskite structure can therefore be represented as linked framework of BO_6 (TiO_6) octahedral with the A-site ion in 12-fold coordination with oxygen and the B-site in 6-fold coordination. In most cases the cubic structure in Fig. 2.8 is somewhat idealed. The structural formula is often referred to as:

$$A^{(XII)}B^{(VI)}X_3^{(VI)} \qquad (2.7)$$

in which the A atoms are in 12-fold coordination and both the B and X atoms are in 6-fold coordination.

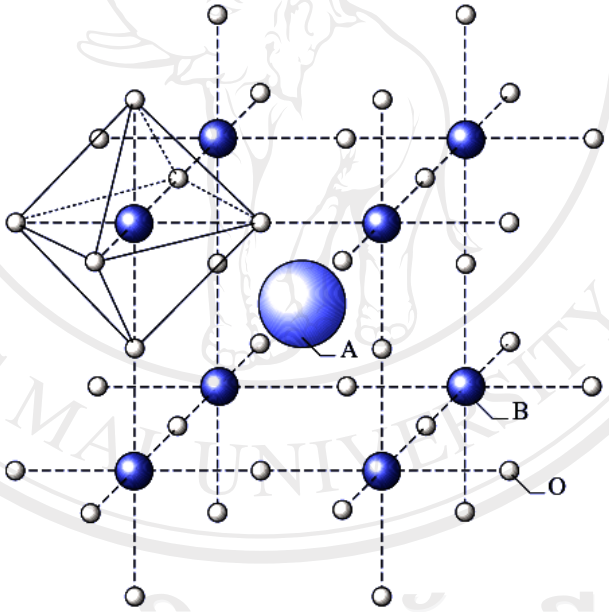

Fig. 2.8 The perovskite crystal structure [8].

The perovskite structure is tolerant of a very wide range of multiple cation substitutions on both the A- and B-sites. The anions and cations can be interchanged with ions of different valences, as long as charge neutrality is maintained. The first of the three major variations is the $A^{1+}B^{5+}O_3$ family, as example of which is $KNbO_3$. The best studied family is probably $A^{2+}B^{4+}O_3$ (Fig 2.9), which include $PbTiO_3$ and $BaTiO_3$. Finally, is $A^{3+}B^{3+}O_3$ family, such as $BiFeO_3$ and $BiScO_3$.

ลิขสิทธิ์มหาวิทยาลัยเชียงใหม่
Copyright © by Chiang Mai University
All rights reserved

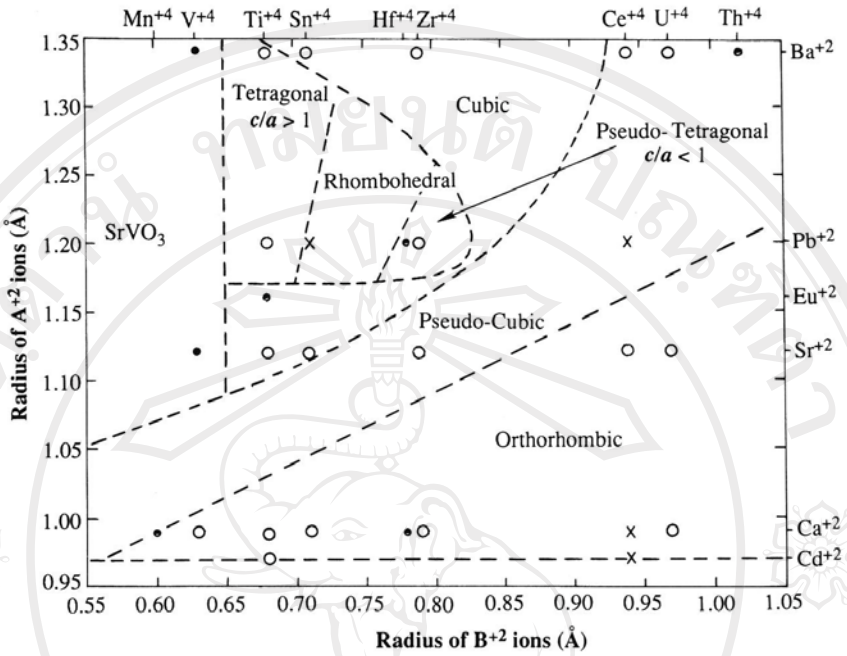

Figure 2.9 Classification of the perovskite $A^{2+}B^{4+}O^{2-}{}_3$ – type compounds according to the constituent ionic radii [19].

In addition to these three families, there are a wide variety of complex perovskite forms resulting from multiple ionic substitutions. The general formula for the complex perovskite is

$$(A'A'')^{(XII)}(B'B'')^{(VI)}X_3{}^{(VI)} \qquad (2.8)$$

The A′ and A″ cation sites typically contain Pb^{2+}, Ba^{2+}, Sr^{2+}, Bi^{2+} or La^{2+}; the X anion site is generally occupied by oxygen; and the B′ and B″ cation sites can contain a great variety of cation. The B′ site is usually occupied by a lower valence cation, such as Mg^{2+}, Ni^{2+}, Zn^{2+}, Fe^{3+} or Sc^{3+}. The B″ site is typically highly-charged ions such as Ti^{4+}, Nb^{5+}, Ta^{5+} or W^{6+}.

ลิขสิทธิ์มหาวิทยาลัยเชียงใหม่
Copyright© by Chiang Mai University
All rights reserved

These substitutions generally lead to there major complex perovskite sub-families: $A^{2+}(B^{3+}_{1/2}B^{5+}_{1/2})O_3$, $A^{2+}(B^{2+}_{1/2}B^{6+}_{1/2})O_3$ and $A^{2+}(B^{2+}_{1/3}B^{5+}_{2/3})O_3$ in Fig 2.10. Most relaxor ferroelectrics are rhombohedral perovskite, however, in many cases the symmetry is described as pseudo-cubic due to a lack of long-range global order [20].

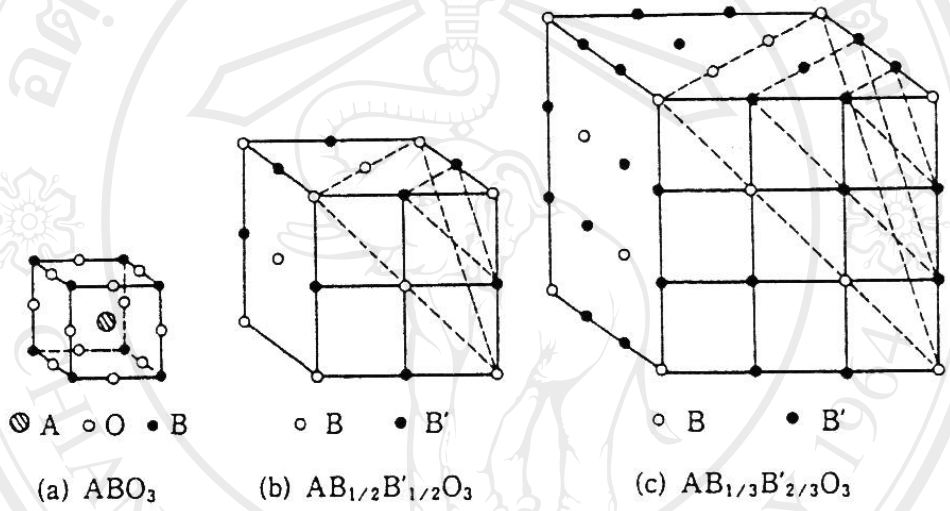

Figure 2.10 Order arrangement of B-site ions in complex perovskites : (a) simple type, (b) 1:1 order type, (c) 1:2 order type [21].

Due to the large number of substitutions that are possible in perovskite structure, Goldschmidt [22] developed a “tolerance” factor to describe the stability limits of the structure. In general, the perovskite structure is formed if the tolerance factor (t), is in the range 0.8-1.0, tolerance factor is calculated based on radii of the A, B and oxygen ions[23], respectively.

$$t = (R_A + R_O)/\sqrt{2}(R_B + R_O) \qquad (2.9)$$

where R is the ionic radius of the A, B or oxide ion

ลิขสิทธิ์มหาวิทยาลัยเชียงใหม่
Copyright© by Chiang Mai University
All rights reserved

Since most perovskites contain lead and barium there is a tendency toward A-O bonding with a strong covalent character. This factor must be considered in determining the stability of the perovskite structure. The percentage of the ionic character of the bonds is proportional to the electronegativity difference between the cation and anion. Halliyal *et al*.[24] developed a structure field map based on the average electronegativity difference between cations and the geometric tolerance factor (Fig. 2.11). The electronegativity differences of cation A and oxygen X_{A-O} and cation B and oxygen X_{B-O} were calculated using Pauling's electronegativity scale. For $A(B'B'')O_3$ type perovskites, a weighted average value was used for calculating r_b and X_{B-O}. The electronegativity difference (ΔEN) is given by the following equation:

$$\Delta EN = \frac{(X_{A-O} + X_{B-O})}{2} \qquad (2.10)$$

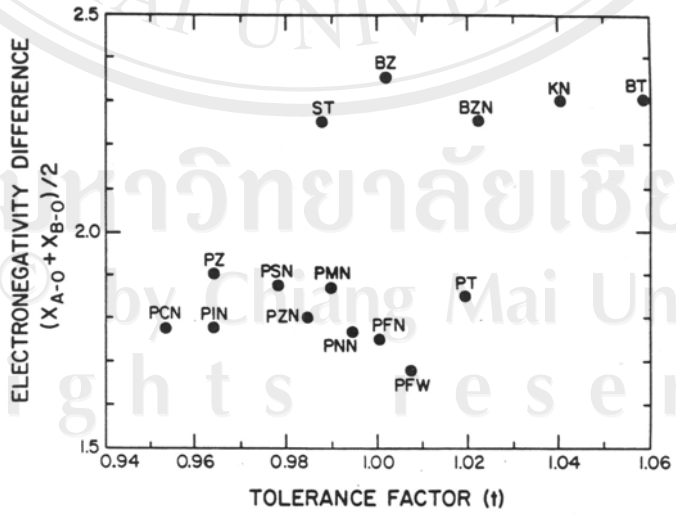

Figure 2.11 Electronegativity difference versus tolerance factor for ABO_3 perovskite compounds [24].

ลิขสิทธิ์มหาวิทยาลัยเชียงใหม่
Copyright© by Chiang Mai University
All rights reserved

2.2.1. Lead zirconate titanate ($Pb(Zr,Ti)O_3$ or PZT)

Due to the strong piezoelectric behavior of lead zirconate titanate, discovered by B. Jaffe in the 1955, it has become the most widely employed piezoelectric material – replacing barium titanate for almost all applications[9].

Piezoelectric ceramics from the $Pb(Zr,Ti)O_3$ [PZT] solid solution system have been widely used because of their superior piezoelectric properties. The phase diagram for the $Pb(Zr_xTi_{1-x})O_3$ system appears in Figure 2.12 [9]. The symmetry of a given composition is determined by the Zr content. Lead titanate also has a perovskite structure and a tetragonally distorted ferroelectric phase. With increasing Zr content, x, the tetragonal distortion decreases and at $x > 0.52$ the structure changes from tetragonal 4mm to another ferroelectric phase with rhombohedral 3m symmetry. The line dividing these two phases is called the *morphotropic phase boundary* [MPB].

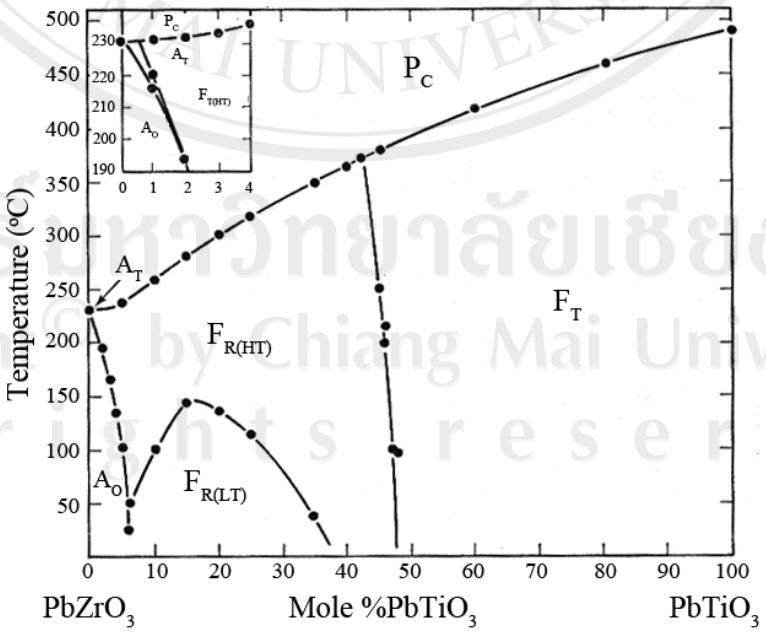

Figure 2.12 $PbTiO_3$-$PbZrO_3$ sun-solidus phase diagram[9].

ลิขสิทธิ์มหาวิทยาลัยเชียงใหม่
Copyright© by Chiang Mai University
All rights reserved

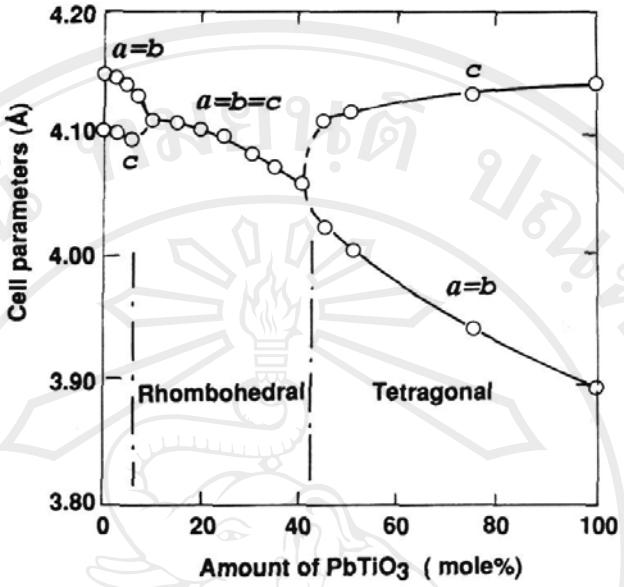

Figure 2.13 Lattice parameters at room temperature for the $PbZrO_3$-$PbTiO_3$ system.

The composition at the morphotropic phase boundary is assumed to be a mixture of the tetragonal and rhombohedral phases. Lattice parameters of PZT are plotted against compositions in Fig. 2.13 [25]. At temperatures below the Curie point, T_c, small displacements of the ions result in a separation of the positive and negative charge creating an electric dipole, which is accompanied by an elongation of the unit cell along the polarization direction. In the tetragonal phase, the polar axis is along one of the 6 <001> directions, and along one of the 8 <111> directions in the rombohedral phase as shown in Figure 2.14 [26]. Application of an electric field can reorient the spontaneous polarization along any of the equivalent directions. The dependence of dielectric constant, elecctromechanical coupling factor, piezoelectric strain coefficients (d) and remanent polarization on composition over a narrow compositional range near the morphotropic phase boundary is shown in Figures 2.15-2.16. All the coefficients are observed to peak at the morphotropic phase boundary.

ลิขสิทธิ์มหาวิทยาลัยเชียงใหม่
Copyright© by Chiang Mai University
All rights reserved

The enhancement in the piezoelectric effect at the morphotropic phase boundary has been attributed to the coexistence of the two phases, whose polarization vectors become more readily aligned by an applied electric field when mixed in this manner than may occur in either of the single phase regions.

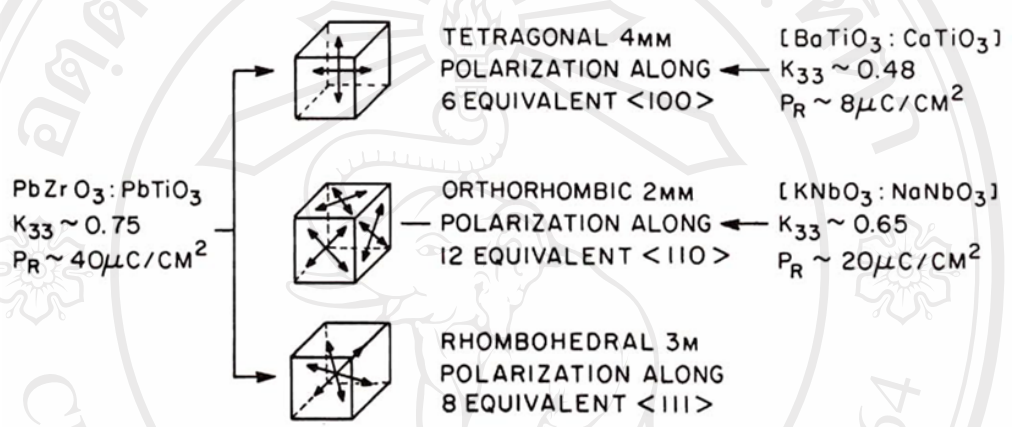

Figure 2.14 Possible orientation state in perovskites [26].

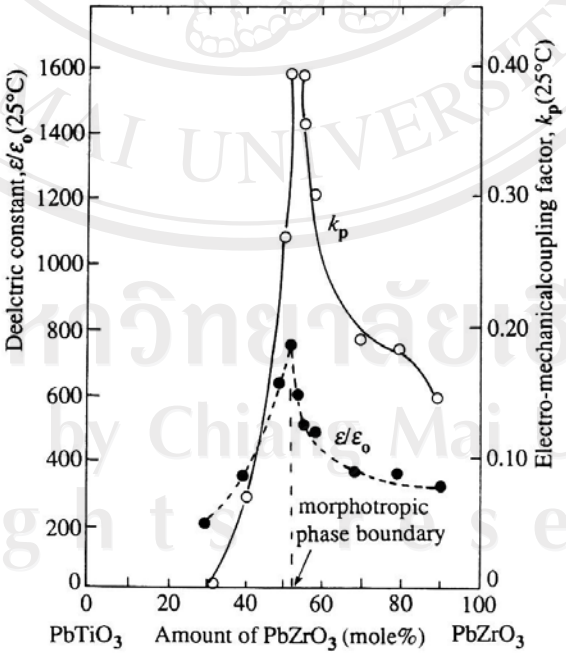

Figure 2.15 Composition dependence of dielectric constant and elecctromechanical coupling factor in PZT system [3].

ลิขสิทธิ์มหาวิทยาลัยเชียงใหม่
Copyright© by Chiang Mai University
All rights reserved

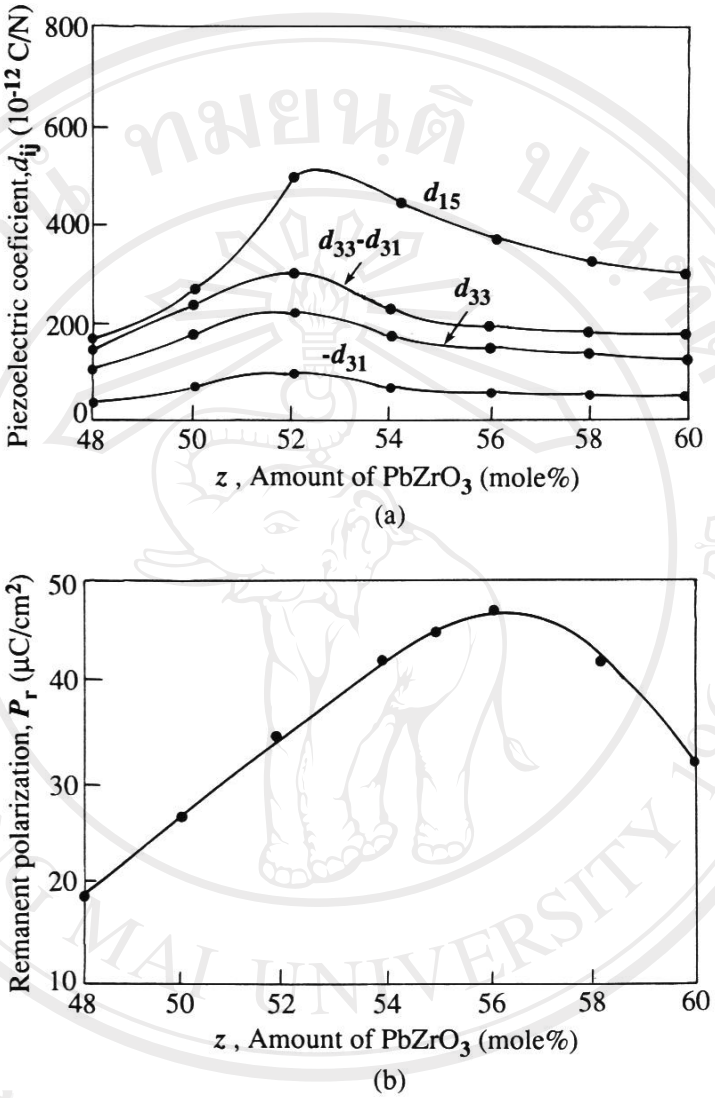

Figure 2.16 (a) Variation of piezoelectric coeffecient d_{ij} and (b) remanent polarization P_r with composition of PZT near the morphotropic phase boundary [9].

ลิขสิทธิ์มหาวิทยาลัยเชียงใหม่
Copyright© by Chiang Mai University
All rights reserved

2.2.2. Modification by doping

In general, the term "doping" of piezoelectric ceramics implies that some ions, whose chemical valence is difference from those of the original ions in the lattice as shown in Fig. 2.17 [27] , or some compounds with a chemical formula $A^{+}B^{5+}O_3^{2-}$ or $A^{3+}B^{3+}O_3^{2-}$, are added to the PZT piezoelectric ceramics. The variation in the

properties of PZT resulting from difference dopings are complicated (as list in Table 2.3) and present in the following paragraphs a details disscusion.

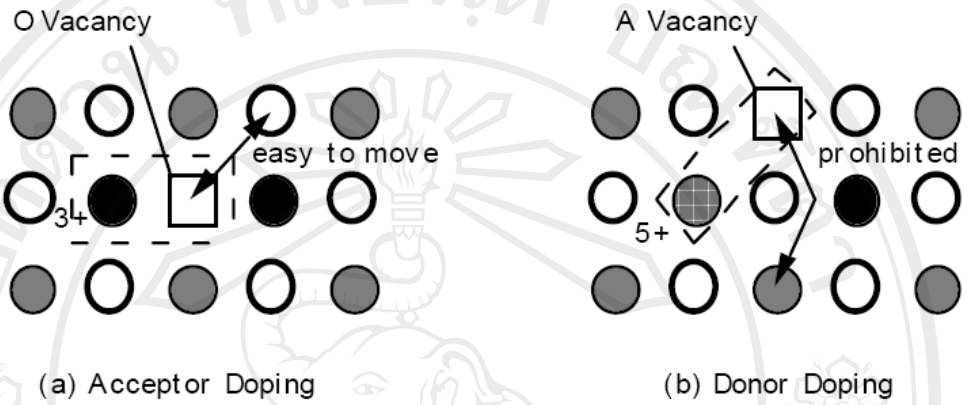

Figure 2.17 Crystal deficiencies in PZT for acceptor (a) and donor (b) dopants [27].

Table 2.3 Common doping effect for PZT ceramics relative to undoped PZT ceramic [28].

Classification	Position for doping	Dopants	Effect
"Soft" PZT	A-site donors	La^{3+}, Bi^{3+}, Nd^{3+}	• Reduces oxygen vacancies. • Increases volume resistivity. • Increases domain wall mobility • High dielectric, piezoelectric constant. • Increases elastic compliance. • High dielectric loss. • Low mechanical quality factor. • Easy poling, low coercive field. • Low aging effect
	B-site donors	Nb^{5+}, Sb^{5+}	
"Hard" PZT	A-site acceptors	K^{+}, Rb^{+}	• Increases oxygen vacancies. • Decreases unit cell volume. • Decreases volume resistivity. • Decreases domain wall mobility • Low dielectric, piezoelectric constant. • High mechanical quality factor. • Low dielectric loss. • High coercive field. • Hard poling and depoling. • High aging effect.
	B-site acceptors	Co^{3+}, Fe^{3+},Sc^{3+}, Ga^{3+},Cr^{3+},Mn^{3+}, Mg^{2+}, Cu^{2+},Al^{3+}	

ลิขสิทธิ์มหาวิทยาลัยเชียงใหม่
Copyright© by Chiang Mai University
All rights reserved

2.2.2.1. Soft doping

Ions for soft doping include La^{3+}, Nd^{3+}, and other rare earth, Sb^{3+}, Bi^{3+}, Th^{4+}, Nb^{5+}, Sb^{5+}, W^{6+}, etc. [29-36]. The doping process is rather straightforward, i.e., metal oxides of these elements are simply added to the raw materials for mixing. A soft doping ion may soften properties of piezoelectric ceramics, i.e., elastic compliance coeffectient s_{ij}, dielectric constant ε_r, k_p and bulk resistivity ρ_v are enhanced, while the coercive filed E_c and Q_m are reduced. As an example of softening doping ions, the variation of k_p in PZT ceramics with various amount of Nb^{5+} doping is shown in Fig. 2.18 [37].

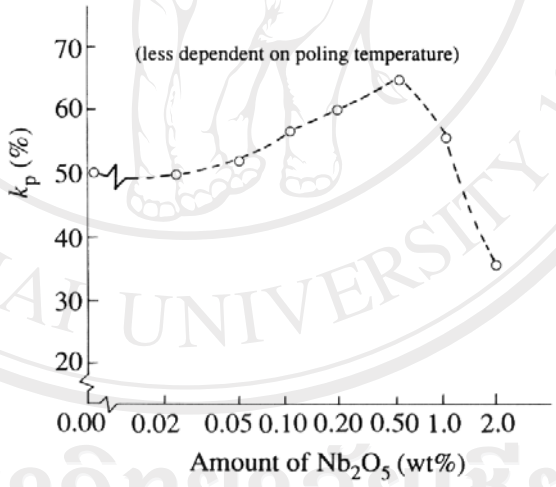

Figure 2.18 Variation of the coupling factor k_p in $Pb(Zr_{0.52}Ti_{0.48})O_3$ piezoelectric ceramics with various doping amounts of Nb_2O_5 [37].

The softening effect of soft doping is attributed to the creation of Pb vacancies in the perovskite lattice when the soft doping ions enter the lattice structure. Since Pb^{2+} ion occupy the A-sites of the perovskite lattice, soft doping ions play a role in causing the A vacancies. In general, ions with larger ionic radii, such as La^{3+}, Nd^{3+},

ลิขสิทธิ์มหาวิทยาลัยเชียงใหม่
Copyright© by Chiang Mai University
All rights reserved

Sb^{3+}, Bi^{3+}, Th^{4+}, etc., occupy the A-sites to replace Pb^{2+} ions. Therefore, extra positive charges are introduced into the lattice due to the fact the valence of the doping ions is higher than that of Pb^{2+} ions. When two A-sites are occupied by two cations with a valence of +3, a Pb vacancy is created in the lattice to maintain electroneutrality.

When ions with smaller ionic radii, such as Nb^{5+}, Ta^{5+}, Sb^{5+}, W^{6+}, etc. enter into the perovskite lattice, they occupy the B-sites to replace Zr^{4+} or Ti^{4+} ions. Since the doping ions have a higher valence than +4, extra positive charges enter the lattice and Pb vacancies have to created to ensure electroneutrality. Ionic radii of some soft doping ions are listed on Table 2.4. In the lattice having Pb vacancies, transfer of atoms is easier than in a perfect lattice; thus domain motions can be caused by the smaller electric field (or a mechanical stress). Thereby, the coercive field of ferroelectric is reduced. Q_m decreases with increasing internal friction (mechanical loss and electrical loss), because more energy is spent in domain and ionic dynamic process.

In soft-doped ceramics, where Pb^{2+} ions are replaced partially by La^{3+} ions, or Ti^{4+} ions partially by Nb^{5+} ions, La^{3+} or Nb^{5+} can play rule of a center of positive electric charges, similar to the donor impurity in semiconductor. This center can attract and bind and electron, which can easily be excited by an electric field. When concentration of donor impurities is close to that of the acceptor originating from Pb vacancies, most of the holes from acceptor level are compensated by electrons from the donors level. As a result, the bulk resistivity of PZT with soft doping increases. Consequencely it becomes easier to establish a high electric field in PZT with soft doping because of its high resistivity value and the domain motion is also easier

ลิขสิทธิ์มหาวิทยาลัยเชียงใหม่
Copyright © by Chiang Mai University
All rights reserved

owing to the existence of Pb vacancies. The combined effect of these two factors, which causes more than adequate realighment of domains directly results in higher piezoelectric activities for soft PZT in composition with those in an undoped PZT.

Table 2.4 Radii of soft dopant ions

Small ions	(Å)	Large ions	(Å)
Ti^{4+}	0.68	Pb^{2+}	1.32
Zr^{4+}	0.79	La^{3+}	1.22
Nb^{5+}	0.69	Nd^{3+}	1.15
Ta^{5+}	0.68	Sb^{3+}	0.90
Sb^{5+}	0.63	Bi^{3+}	1.14
W^{6+}	0.65	Th^{4+}	1.10

2.2.2.2. Hard doping

Hard doping ions on PZT include K^{+}, Na^{+}, which occupy the A-sites and Fe^{2+}, Fe^{3+}, Co^{2+}, Co^{3+}, Mn^{2+}, Mn^{3+}, Ni^{2+}, Mg^{2+}, Al^{3+}, Ga^{2+}, In^{3+}, $Cr^{3+}$and Sc^{3+}, which occupy the B-sites in the perovskite strucuture [30-31, 37-40]. In the process of doping, metal oxide of these elements are usually directly added to the raw materials to mixing. Unlike soft doping, hard doping increases the hardness pf PZT properties, i.e. lower dielectric constant, lower dielectric loss, higher coercive field, higher Q_m, a slightly lower $k_{p,}$ and a lower bulk resistivity. Physical mechanisms of hard doping are complex, because different hard doping ions affect different properties. For example, a ternary ceramics system with Mn^{2+} doping have an enhanced Q_m and almost unchanges k_p as shown in Fig 2.19 [41]. In PZT with Fe^{3+} doping, the dielectric loss is usually reduced. This is especially true of the dielectric loss in the

ลิขสิทธิ์มหาวิทยาลัยเชียงใหม่
Copyright© by Chiang Mai University
All rights reserved

strong external field, as shown in Fig 2.20 [38]. Therefore, Fe^{3+} ion is an effective hard doping ion for PZT used in high-power transducer.

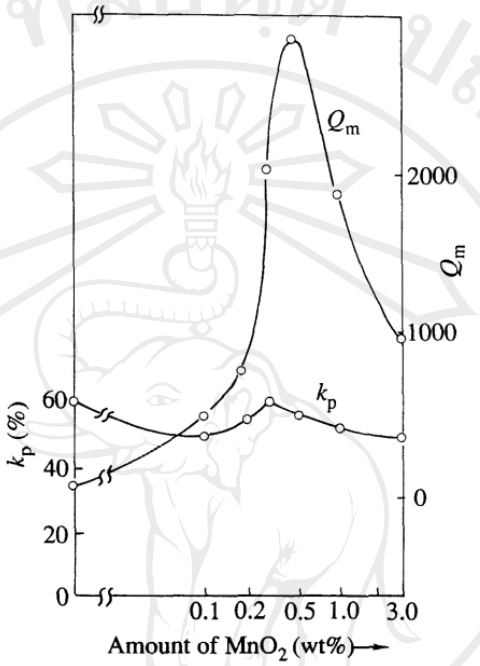

Figure 2.19 Variation of the piezoelectric properties in the $0.05Pb(Sc_{1/2}Ta_{1/2})O_3$-$0.455PbTiO_3$-$0.495PbZrO_3$ ceramics with various doping amounts of MnO_2 [41]

A hard doping ion is considered an acceptor, since it causes oxygen vacancies in the perovskite lattice. Both the A-sites and the B-sites may be occupied by the hard doping ion. Which one of these is occupied depends on the ionic radius of the doping ion, which usually has a lower chemical valence than of the ion replaced in the lattice. Foe example, Pb^{2+} ions may be replaced by K^{+} ions and Zr^{4+} (or Ti^{4+}) ions by Fe^{3+}, Sc^{3+} or Mg^{2+}. Table 2.5 lists ionic radii of selected hard doping ions.

ลิขสิทธิ์มหาวิทยาลัยเชียงใหม่
Copyright © by Chiang Mai University
All rights reserved

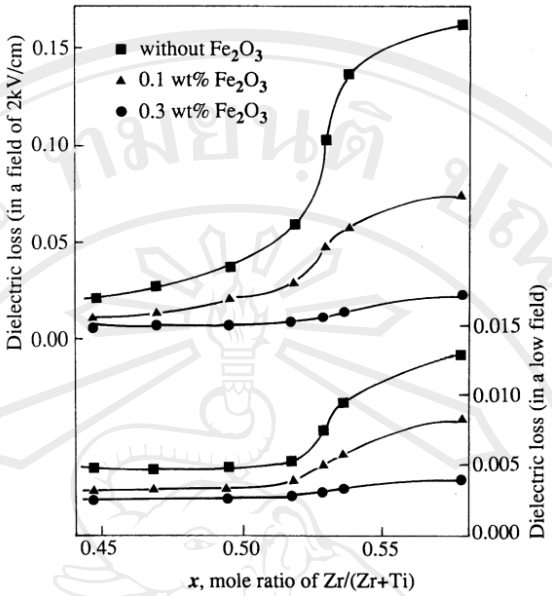

Figure 2.20 Variation of the dielectric loss in a PZT piezoelectric ceramics with difference doping amounts of Fe_2O_3 [38]

Table 2.5 Radii of hard dopant ions

Small ions	(Å)	Large ions	(Å)
Ti^{4+}	0.68	Pb^{2+}	1.32
Zr^{4+}	0.79		
Fe^{3+}	0.67	K^{+}	1.33
Al^{3+}	0.57	Na^{+}	0.94
Sc^{3+}	0.83		
In^{3+}	0.92		
Cr^{3+}	0.64		

When hard doping ions with lower positive valence replace metal ions with higher positive valence, oxygen vacancies are created in the lattice, on account of the requirements of electroneutrality. For example, when two Pb^{2+} ions may be replaced by two K^{+} ions, or when two Zr^{4+} (or Ti^{4+}) ions by two Fe^{3+}ion, one oxygen vacancy

ลิขสิทธิ์มหาวิทยาลัยเชียงใหม่
Copyright© by Chiang Mai University
All rights reserved

is created. Thus, two hard doping ions may cause the creation of one oxygen vacancy, which cannot be removed by sintering the ceramic in the atmosphere of oxygen. The perovskite structure is composed of oxygen octahedra, and to maintain the stability of the oxygen octahedron framework, the oxygen vacancy concentration of oxygen vacancy in the lattice have been observed. An undoped PZT ceramics has p-type electrical conduction mechanism. Therefore, in a PZT ceramics with hard doping ions, space charges (i.e., both centers of negative charges and hole- carriers) increase dramatically. These space charge causes an internal field in side the grains of PZT, and this field may inhibit domain motion. For poling a hard ceramic, higher poling temperatures are usually necessary. When the temperature is higher, space charges move more freely because of the decrease in the bulk resistivity of the ceramic. Subsequently, the reduction in the space-charge accumulation allows easier domain motion. As an example, k_p of PZT ceramics is plotted as a function of the amount of Cr_2O_3 doping at different poling temperature in Fig 2.21 [42]. It shows that the enhancement of the poling temperature enhances the piezoelectric activity as well.

Hard doping ions also inhibit grain growth due to the low solubilities of these ions in the lattice of the solid solution. As a result, a portion of the doping oxides precipitate out of the normal grain and stay at grain boundaries which subequently resist the grain growth. Another effect of these precipitates is that they accumulate in the grain boundaries as bound binding the adjacent grain and thus enhance the elastic stiffness content as well as strength, has been reported in Fe_2O_3 (or Cr_2O_3) doped ceramics [31].

ลิขสิทธิ์มหาวิทยาลัยเชียงใหม่
Copyright© by Chiang Mai University
All rights reserved

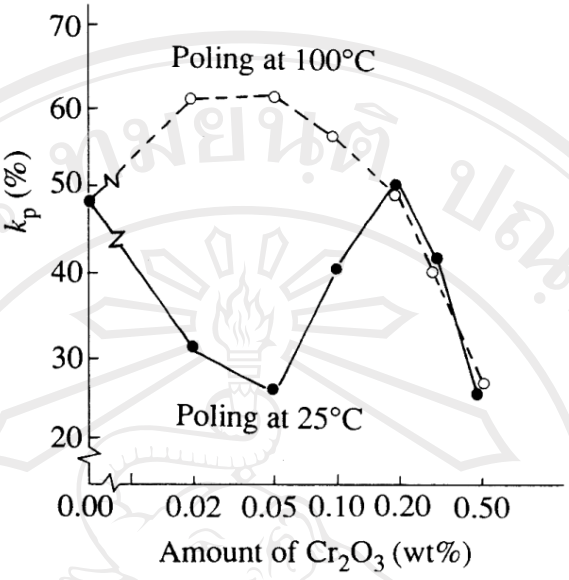

Figure 2.21 Effect of poling temperature on the coupling factor k_p in the $Pb(Zr_{0.52}Ti_{0.48})O_3$ piezoelectric ceramics with various doping amounts of Cr_2O_3 [42]

2.2.2.3. Other doping ions

Some doping ions, such as ions of cerium, chromium and uranium, in piezoelectric ceramics play the role of both a softener and a hardener. PZT ceramics with Ce doping possess a high bulk resistivity, a higher Q_m ,ε_{mn} and E_c. These ceramics can be poled by applying higher electric fields at higher poling temperatures because of their high resistivities, and higher k_p are obtained. These materials also have high ageing resistance, good thermal stability and are relative more stable in strong in strong fields. In addition, Ce doping help the grain growth [43].

Usually, doping of Cr is considered as hard doping. However , as a dopant, Cr is difference from the other hard doping ions. A Cr-doped PZT ceramic has a high Q_m and enhanced stability, while its dielectric loss increases and its k_p decreases. The effect of Cr on the bulk resistivity is complex . That believed to be an effect of Cr ion

ลิขสิทธิ์มหาวิทยาลัยเชียงใหม่
Copyright© by Chiang Mai University
All rights reserved

accumulation at grain boundaries, which would cause the electrical conductivity of PZT to increase [31].

Doping of U in PZT results in a higher Q_m (especially in trigonal phase PZT), a higher resistivity, better aging characteristics and higher dielectric loss. PZT ceramics with Ag, Ir or Rh doping apparently have a high k_p and Q_m, and a slightly lower dielectric constant.

Complexed doping, doping with two or more metal elements, is frequently used for better results. As an example, Fig 2.22 shows that in the ternary piezoelectric ceramics $Pb(Zn_{1/3}Nb_{2/3})O_3$-$PbTiO_3$-$PbZrO_3$, the effect of complexed doping of both NiO and MnO_2 is better that of single doping of MnO_2. Another example is complex doping of Ce and Mn; the thermal stability of doped piezoelectric ceramics is improved drastically.

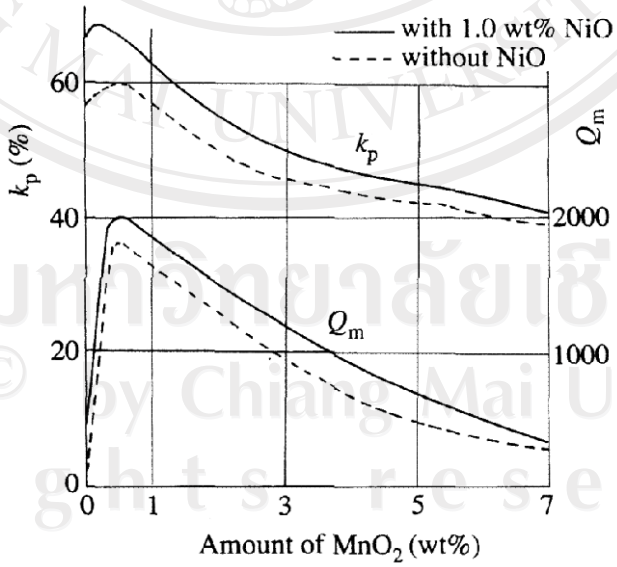

Figure 2.22 Effect of complex doping of both NiO and MnO_2 on the piezoelectric properties of the $Pb(Zn_{1/3}Nb_{2/3})_{0.2}Ti_{0.36}Zr_{0.44}O_3$ ceramics [44]

ลิขสิทธิ์มหาวิทยาลัยเชียงใหม่
Copyright© by Chiang Mai University
All rights reserved

2.2.2.4. Hard and soft piezoelectrics

Small amounts of dopants sometimes drastically change the dielectric and electromechanical properties of ceramics. Donor doping tends to facilitate domain wall motion, leading to enhanced piezoelectric charge coefficients (*d*), and electromechanical coupling factors (*k*), producing what is referred to as a "soft piezoelectric." Acceptor doping, on the other hand, tends to pin domain walls and impeding their motion, leading to an enhanced mechanical quality factor (Q_m), producing what is called a "hard piezoelectric." Table 2.6 summarizes the advantages and disadvantages of soft and hard piezoelectrics and compares their characteristics with a leading electrostrictive material, $Pb(Mg_{1/3}Nb_{2/3})O_3$ (PMN). The electrostrictive ceramic is commonly used for positioning devices where hysteresis-free performance is a primary concern. However, due to their high permittivity, the electrostrictive devices are generally used only for applications that require slower response times.

On the other hand, the soft piezoelectric materials with their relatively low permittivity and high piezoelectric charge coefficients, *d*, can be used for applications requiring a quick response time, such as pulse driven devices like inkjet printers. Soft piezoelectrics generate a significant amount of heat when driven at resonance, however, due to their small mechanical quality factor, Q_m. Thus, for ultrasonic motor applications, hard piezoelectrics with a larger mechanical quality factor are preferred despite the slight sacrifices incurred with respect to their smaller piezoelectric strain coefficients, *d*, and the electromechanical coupling factors, *k*.

ลิขสิทธิ์มหาวิทยาลัยเชียงใหม่
Copyright© by Chiang Mai University
All rights reserved

Table 2.6 Advantages (+) and disadvantages (−) of soft and hard piezoelectrics, compared with the features of a leading electrostrictive material, $Pb(Mg_{1/3}Nb_{2/3})O_3$ (PMN) [45].

	d	k	Q_m	Off -Resonance Application	Resonance Application
Electrostrictor (PMN)	+	+	-	**High displacement No hysteresis**	**Wide band**
Soft Piezo (PZT-5H)	+	+	-	**High displacement ($\Delta L = dEL$)**	***Heat generation**
Hard Piezo (PZT- 8)	-	-	+	***Low strain**	**High AC displacement ($\Delta L \propto Q_m.dEL$)**

*** Demerit**

2.2.3. Modification by relaxor ferroelectric

The high properties in PZT being related to the presence of a morphotropic phase boundary, it was natural to look for other perovskite compounds exhibiting a similar feature. For instance, solid solutions of lead hafnate titanate were tested and indeed exhibited a MPB with enhanced properties [46] but not sufficiently elevated to compete with PZT. A significant increase in properties came from the mixing of relaxor ferroelectrics (such as $Pb(Mg_{1/3}Nb_{2/3})O_3$ (PMN) , $Pb(Zn_{1/3}Nb_{2/3})O_3$ (PZN), $Pb(Ni_{1/3}Nb_{2/3})O_3$ (PNN)) with normal ferroelectrics such as PT or PZT. These compounds form a solid solution which typically follows the typical ternary diagram presented in Fig. 2.23. Various ternary solid solutions incorporating PZT and another ferroelectric perovskite have also been investigated. Some noteworthy examples utilize the following third phases as presented in Table 2.7. Possible range of planar

ลิขสิทธิ์มหาวิทยาลัยเชียงใหม่
Copyright © by Chiang Mai University
All rights reserved

coupling k_p and mechanical quality factor Q_m for modified PZT and ternary composition is shown in Fig 2.24.

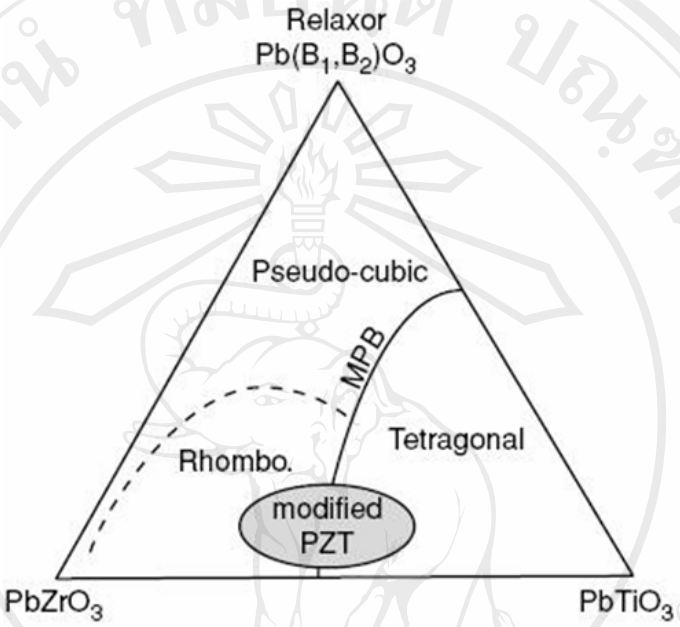

Figure 2.23 Ternary diagram depicting MPBs in $Pb(Zr,Ti)O_3$ and relaxor ferroelectric systems for piezoelectric ceramics [46].

Table 2.7 Ternary piezoelectric ceramics compositions [47].

□ -$PbZrO_3$- $PbTiO_3$

$(A^{1+}_{1/2}A^{3+}_{1/2})TiO_3$	$Pb(B^{2+}_{1/3}B^{5+}_{2/3})O_3$	$Pb(B^{3+}_{1/2}B^{5+}_{1/2})O_3$
$Pb(B^{2+}_{1/2}B^{6+}_{1/2})O_3$	$Pb(B^{3+}_{2/3}B^{6+}_{1/3})O_3$	$Pb(B^{1+}_{1/4}B^{5+}_{3/4})O_3$

A^{1+} : Li, Na, K
A^{3+} : Bi, La, Ce, Nd
B^{1+} : Li, Cu
B^{2+} : Mg, Ni, Zn, Mn, Co, Sn, Fe, Cd
B^{3+} : Mn, Sb, Al, Yb, In, Fe, Co, Sc
B^{5+} : Nb, Sb, Ta, Bi
B^{6+} : W, Te, Re

ลิขสิทธิ์มหาวิทยาลัยเชียงใหม่
Copyright© by Chiang Mai University
All rights reserved

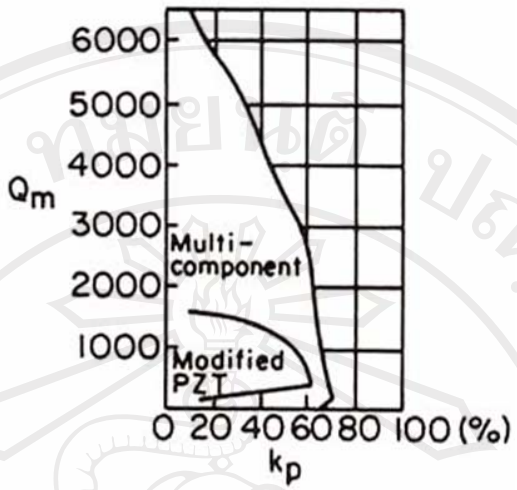

Figure 2.24 Possible range of planar coupling k_p and mechanical quality factor Q_m for modified PZT and ternary composition[46].

Those solid solutions present a MPB which is dependent on the relaxor content. Such MPB compositions, and in particular the binary ones between PT and relaxors, exhibit very high properties. Although the Curie temperatures are quite low for the relaxor-ferroelectric solid solutions reported above, their superior dielectric and piezoelectric properties are very attractive. Hence, a compromise is necessary between T_C decrease and properties improvement. Nowadays, these compositions (and their compounds with PZ) are among the most interesting soft ferroelectrics for piezoelectric applications [48]

2.2.4. Lead zinc niobate ($Pb(Zn_{1/3}Nb_{2/3})O_3$ or PZN)

Lead zinc niobate, $Pb(Zn_{1/3}Nb_{2/3})O_3$, or PZN, is one of the first known relaxor perovskite ferroelectrics reported by Bokov and Mylnikova in 1960 [49] which shows excellent dielectric, electrooptic, and electrostrictive properties[50-52]. Because of the partially disordered arrangement of the Zn^{2+} and Nb^{5+} cations in the B-site of the

ลิขสิทธิ์มหาวิทยาลัยเชียงใหม่
Copyright© by Chiang Mai University
All rights reserved

perovskite structure, a broad ferroelectric phase transition from rhombohedral (ferroelectric) to cubic (paraelectric) symmetry takes place at about 140°C, showing a very high dielectric constant maximum [53]. Extensive research has been carried out on PZN single crystals because of their excellent dielectric, electrostrictive, and optical properties. The solid solution between PZN with a rhombohedral system and $PbTiO_3$ (PT) with tetragonal symmetry has a morphotropic phase boundary near 9 mol% PT [54]. Single crystals with a composition near the MPB show extremely large dielectric ($\varepsilon_r \sim 60{,}000$) and piezoelectric coefficients, and are much larger than those of PZT ceramics. Single crystals of the MPB composition (0.91PZN-0.09PT) display one of the highest electromechanical coupling factors (0.92) and piezoelectric coefficients (1500 pC/N) at room temperature. Because of the high Curie temperature and the low sintering temperature (1050-1100^{o}C), PZN-based compositions are promising ferroelectrics for device applications.

Although single crystals of PZN can be routinely grown by the flux method, it is known that perovskite PZN ceramics cannot be synthesized by the conventional mixed-oxide method without doping [24, 55-56]. This is because PZN has a low tolerance factor and small electronegativity difference between the cations and the pyrochlore phase appears to be more thermodynamically stable than the perovskite phase. Attempts to synthesize perovskite PZN ceramics invariably result in the formation of a pyrochlore phase with accompanying degradation of the dielectric and piezoelectric properties. When the normal solid state reaction is carried out to prepare PZN, a mixture of perovskite PZN and pyrochlore-type $Pb_3Nb_4O_{13}$ or $Pb_2Nb_2O_7$ is

ลิขสิทธิ์มหาวิทยาลัยเชียงใหม่
Copyright© by Chiang Mai University
All rights reserved

formed [57]. The anion-deficient, cubic pyrochlore, $Pb_3Nb_4O_{13}$, is the most common; however, both phases can be present. $Pb_2Nb_2O_7$ is a rhombohedral pyrochlore that is also sometimes present. The pyrochlore phase is undesirable because of its relatively low dielectric constant (~200) and non-piezoelectric nature.

A reaction sequence for pyrochlore formation in PMN has been proposed by Lejeune *et.al*. [58] In this reaction, PbO and Nb_2O_5 react first to form cubic pyrochlore. Further reaction with PbO results in the formation of a rhombohedral pyrochlore. At high temperatures, the rhombohedral pyrochlore reacts with MgO to form perovskite PMN, with the reappearance of cubic pyrochlore. A similar reaction is believed to occur in PZN-based ceramics [59].

The columbite method was suggested by Swartz and Shrout [60] for the preparation of perovskite $Pb(Mg_{1/3}Nb_{2/3})O_3$ (PMN) ceramic. Zinc niobate ($ZnNb_2O_6$, ZN) which is one of the binary niobate compounds with excellent dielectric properties at microwave frequencies [61-63] is well established as the columbite key precursor for the successful preparation of single-phase ferroelectric perovskite PZN based ceramics. However, it is not effective in suppressing pyrochlore phase formation in PZN ceramics.

Many attempts have been made to prepare pyrochlore-free PZN ceramics including synthesis under high pressure condition [64] sol–gel processing [65] and forming solid solutions with more stable perovskites. This last method seems to be the most promising. The stability of modified PZN depends both on the added amount of perovskite compound and on the A- or B-site cation replacement. In this sense, PZN ceramics with 100% perovskite structure can be prepared by adding 6–7 mol%

ลิขสิทธิ์มหาวิทยาลัยเชียงใหม่
Copyright© by Chiang Mai University
All rights reserved

of $BaTiO_3$ [66] or 10% mol of $SrTiO_3$ [56] or PZT [67-68], whereas for $PbTiO_3$ additions (replacement of B-site cations only) the perovskite phase is stable only when the $PbTiO_3$ content exceeds 25 mol%. With these additions the steric hindrance of the lone pair of Pb^{2+} in the perovskite lattice and the mutual interactions between lone pair and Zn^{2+} cations are decreased because of the partial substitution of A- or B-site cations.

Recent work by Fan and Kim [69] has shown that the perovskite phase of $Pb(Zn_{1/3}Nb_{2/3})O_3$ (PZN) ceramics was stabilized by adding a Ti-rich side tetragonal phase of $Pb(Zr_{0.47}Ti_{0.53})O_3$ (PZT) located across the morphotropic phase boundary (MPB). When 40% PZT was added, a rhombohedral perovskite phase was formed without any trace of the pyrochlore phase. The rhombohedral phase fraction decreased markedly with increasing PZT concentration. This work has shown promise in producing pure perovskite phase PZN–PZT ceramics with the conventional mixed-oxide method, making the perovskite phase structure stable, and giving the significantly improved piezoelectric properties.

Vittayakorn *et al.* [70] has studied processing conditions of phase-pure perovskite PZN–PZT ceramics with the conventional mixed-oxide method and B-site precursor. The resulting ceramics displayed excellent dielectric, piezoelectric, and ferroelectric properties in compositions close to the morphotropic phase boundary (MPB). It was also consistently shown that an MPB exists around $x = 0.25$ in this binary system. Excellent piezoelectric properties were found in *0.3*PZN–*0.7*PZT, the composition closest to the MPB with a rhombohedral structure.

ลิขสิทธิ์มหาวิทยาลัยเชียงใหม่
Copyright © by Chiang Mai University
All rights reserved

2.3. Figures of merit in piezoelectrics

There are some important figures of merit in piezoelectrics [7]: the piezoelectric strain constant d, the piezoelectric voltage constant g, the electromechanical coupling factor k and the mechanical quality factor Q_m. These figures of merit are considered in this section.

Piezoelectric Strain Constant d

The magnitude of the induced strain x by an external electric field E is represented by this figure of merit (an important figure of merit for actuator applications:

$$x = dE \tag{2.11}$$

Piezoelectric Voltage Constant g

The induced electric field E is related to an external stress X through the piezoelectric voltage constant g (an important figure of merit for sensor applications):

$$E = gX \tag{2.12}$$

Taking into account the relation, $P = dX$, we obtain an important relation between g and d : $g = \frac{d}{\varepsilon_0 \varepsilon}$ (ε : permittivity) (2.13)

ลิขสิทธิ์มหาวิทยาลัยเชียงใหม่
Copyright© by Chiang Mai University
All rights reserved

Electromechanical Coupling Factor k

The terms, electromechanical coupling factor, energy transmission coefficient, and efficiency are sometimes confused. All are related to the conversion rate between electrical energy and mechanical energy, but their definitions are different.

$$k^2 = \frac{\text{Stored mechanical energy}}{\text{Input electrical energy}} \tag{2.14}$$

or

$$k^2 = \frac{\text{Stored electrical energy}}{\text{Input mechanical energy}} \tag{2.15}$$

Let us calculate Eq. (2.14), when an electric field E is applied to a piezoelectric material. Since the input electrical energy is $\frac{1}{2}\varepsilon_o \varepsilon E^2$ per unit volume and the stored mechanical energy per unit volume under zero external stress is given by

$$\frac{1}{2}\left(\frac{x^2}{s}\right) = \frac{1}{2}\left(\frac{(dE)^2}{s}\right) \tag{2.16}$$

k^2 can be calculated as

$$k^2 = \frac{\frac{1}{2}\left((dE)^2 / s\right)}{\frac{1}{2}\varepsilon_o \varepsilon E^2} = \frac{d^2}{\varepsilon_o \varepsilon\, s} \tag{2.17}$$

Mechanical Quality Factor Q_m

The mechanical quality factor, Q_m, is a parameter that characterizes the sharpness of the electromechanical resonance spectrum. When the motional admittance Y_m is plotted around the resonance frequency ω_0, the mechanical quality factor Q_m is defined with respect to the full width at $Y_m/\sqrt{2}$ [$2\Delta\omega$] as :

$$Q_m = \omega_0 / 2\Delta\omega. \tag{2.18}$$

Also note that Q_m^{-1} is equal to the mechanical loss ($\tan \delta_m$). The Q_m value is very important in evaluating the magnitude of the resonant strain. The vibration amplitude at an off-resonance frequency (dEL, L: length of the sample) is amplified

ลิขสิทธิ์มหาวิทยาลัยเชียงใหม่
Copyright © by Chiang Mai University
All rights reserved

by a factor proportional to Q_m at the resonance frequency. For a longitudinal vibration rectangular plate through d_{31}, the maximum displacement is given by $(8/\pi^2)\, Q_m d_{31} E\, L$.

2.4. Drive/Control Techniques

Piezoelectric/electrostrictive actuators may be classified into two categories, based on the type of driving voltage applied to the device and the nature of the strain induced by the voltage (Figure 2.25 [45]): (1) rigid displacement devices for which the strain is induced unidirectionally along the direction of the applied DC field, and (2) resonating displacement devices for which the alternating strain is excited by an AC field at the mechanical resonance frequency (ultrasonic motors). The first can be further divided into two types: servo displacement transducers (positioners) controlled by a feedback system through a position-detection signal, and pulse drive motors operated in a simple on/off switching mode, examplified by dot-matrix printers. The material requirements for these classes of devices are somewhat different, and certain compounds will be better suited to particular applications. The ultrasonic motor, for instance, requires a very hard piezoelectric with a high mechanical quality factor Q_m, to suppress heat generation. Driving the motor at the antiresonance frequency, rather than at resonance, is also an intriguing technique to reduce the load on the piezoceramic and the power supply. The servo displacement transducer suffers most from strain hysteresis and, therefore, a PMN electrostrictor is used for this purpose. The pulse drive motor requires a low permittivity material aimed at quick response with a certain power supply rather than a small hysteresis, so soft PZT piezoelectrics are preferred rather than the highpermittivity PMN for this application.

ลิขสิทธิ์มหาวิทยาลัยเชียงใหม่
Copyright© by Chiang Mai University
All rights reserved

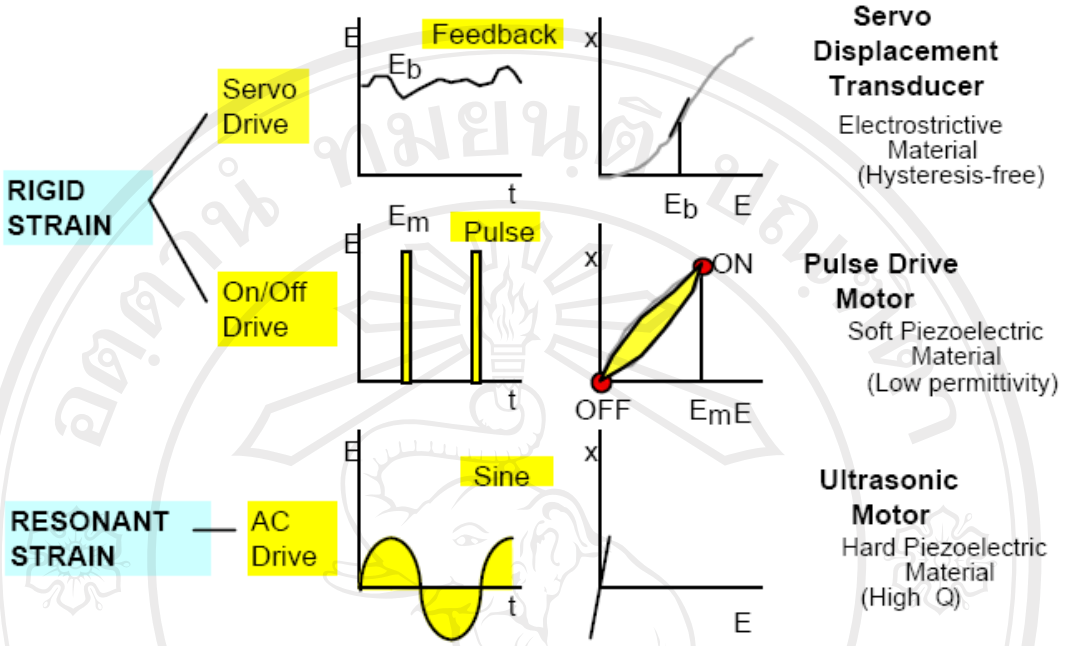

Figure2.25 Classification of piezoelectric/electrostrictive actuators [45].

ลิขสิทธิ์มหาวิทยาลัยเชียงใหม่
Copyright© by Chiang Mai University
All rights reserved